

Mechanistic insights into acidification-augmented coagulation: optimizing cyanobacterial removal and disinfection by-products control

Xin Chen ^{a,b,c,1}, Yunlu Jia ^{a,c,1}, Lili Li ^{a,c}, Jun Ma ^d, Xuezhi Zhang ^{a,c}, Haiyang Zhang ^{a,c,*}

^a Institute of Hydrobiology, Chinese Academy of Sciences, Wuhan, 430072, China

^b University of Chinese Academy of Sciences, Beijing, 100049, China

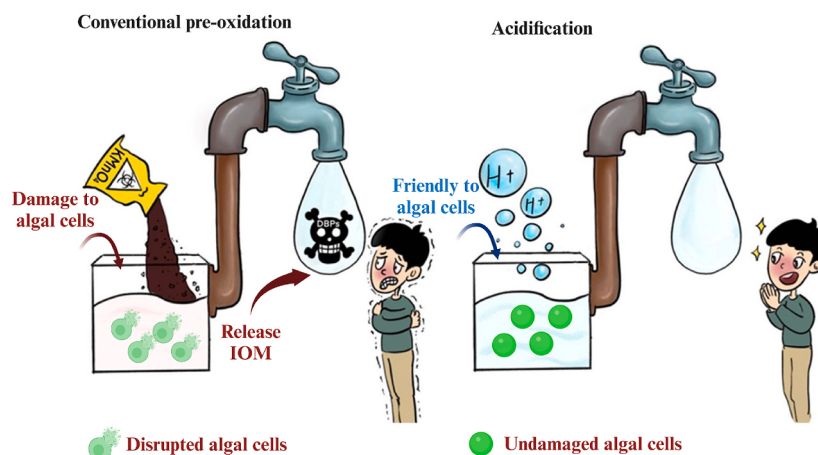
^c Key Laboratory of Algal Biology, Institute of Hydrobiology, Chinese Academy of Sciences, Wuhan, 430072, China

^d State Key Laboratory of Urban Water Resource and Environment, School of Environment, Harbin Institute of Technology, Harbin, 150090, China

HIGHLIGHTS

- Novel acid-coagulation method removes 90 % algae using 60 % less coagulant.
- Brief acidification minimizes cell damage, reducing DBPs formation risk by 30 %.
- Over 50 % decrease in low-polarity AOM components post-acidification.
- AOM composition shift drives charge decrease, enhancing coagulation.

GRAPHICAL ABSTRACT



ARTICLE INFO

Keywords:

Cyanobacteria removal
Enhanced coagulation
Pre-oxidation
Acidification
Disinfection by-products

ABSTRACT

This study develops an acidification-enhanced coagulation (AEC) strategy that selectively modulates algal organic matter (AOM) through pH-controlled interfacial engineering. By implementing mild acid pretreatment (pH 5), the process specifically targets AOM, inducing 54.1 % and 51.7 % reduction of low-polarity proteins and polysaccharides via electrostatic-mediated aggregation, revealed by FT-ICR-MS analysis. The resultant insoluble polymer formation eliminates competitive coagulant-AOM interactions while maintaining cell integrity, contrasting with conventional pre-oxidation that triggers cellular damage. Mechanistic studies reveal the critical role of protonation in modifying AOM's surface charge distribution, thereby enabling effective separation through charge neutralization. At optimal conditions, AEC achieves 60 % coagulant savings and concurrently reduces disinfection by-products (DBPs) formation potential by 30 % (compared with traditional coagulation). The dual

* Corresponding author. Institute of Hydrobiology, Chinese Academy of Sciences, Wuhan, 430072, China.

E-mail address: hyzhang@ihb.ac.cn (H. Zhang).

¹ Equally contributed.

mechanism of selective AOM removal and cell integrity maintaining positions this pH-responsive strategy as a sustainable alternative for drinking water treatment plants combating cyanobacterial blooms, particularly in scenarios requiring minimized chemical footprint and enhanced process safety.

1. Introduction

The intensification of global warming and anthropogenic eutrophication has triggered a surge in harmful cyanobacterial blooms (cyanohABs) across global freshwater systems, with over 21,878 lakes worldwide now experiencing seasonal blooms in the last 40 years (Hou et al., 2022). These blooms may release toxic metabolites (e.g., microcystins) and organic matter, compromising aquatic ecosystem health and drinking water safety (Feng et al., 2024). Addressing increasing cyanobacteria in drinking water sources requires identifying effective removal methods within existing treatment processes to prevent safety incidents and ensure water security.

Current drinking water treatment predominantly relies on coagulation-sedimentation/flotation processes to remove cyanobacterial cells and particulates (Grzegorzek et al., 2023). Since coagulation efficiency dictates subsequent removal performance, achieving optimal results requires coagulant-induced formation of large flocs containing nearly all algal cells with minimal free residuals (Ren et al., 2022). While pre-oxidation enhancement (e.g., potassium permanganate/ozone) ensures cyanobacteria removal during blooms (He et al., 2021; Lin et al., 2016), excessive oxidant dosing frequently triggers cell rupture, releasing intracellular organic matter that elevates cyanobacteria-derived disinfection by-products (DBPs) risks (Dong et al., 2021).

Research confirms algal organic matter (AOM) as the primary coagulation inhibitor (Xu et al., 2018), with extracellular algal-derived organic matter (EOM) occupying coagulant charge sites (Zang et al., 2020) and requiring 4–20 times higher coagulant doses at 5–26 mg C·L⁻¹ concentrations. While isolated cyanobacterial cells achieve effective coagulation with minimal dosing, intracellular algal-derived organic matter (IOM) released during non-selective pre-oxidation exerts 3 times stronger coagulation suppression than EOM at equivalent concentrations (Wang et al., 2022). Paradoxically, oxidative treatments intended to enhance coagulation instead trigger cell rupture, escalating IOM release and coagulant demand in a self-defeating cycle.

Thus, targeted enhancement of cyanobacteria coagulation requires selective neutralization of AOM's inhibitory effects, specifically by blocking its negatively charged functional groups (e.g., carboxyls) that preferentially bind coagulants' positive charge sites (Zang et al., 2020). Research shows reducing these charged groups or altering their dissociation state to neutral enables coagulants to directly engage cyanobacterial cells, achieving effective floc formation without indiscriminate pre-oxidant overuse. This precision strategy contrasts with conventional oxidative dose escalation, which risks cell rupture, amplified IOM release, and elevated DBPs formation, ultimately exacerbating the coagulation inefficiencies it aims to resolve (Reid et al., 2023).

Therefore, this study introduces a non-oxidative strategy to enhance cyanobacteria flocculation by structurally modulating AOM's inhibitory components. Through targeted adjustment of AOM's molecular configuration and functional group dissociation states, the capacity to occupy coagulant binding sites is reduced via charge-based interference. By redirecting coagulants toward cyanobacterial cell interactions rather than AOM sequestration, this approach achieves dual optimization: 1) improved flocculation efficiency through enhancing coagulant-cell interaction efficiency, and 2) mechanistic clarification of charge-shielding effects. The methodology offers a pre-oxidation-free solution for cyanohABs control in water treatment, simultaneously minimizing DBPs formation risks by avoiding cell rupture-induced organic matter release.

2. Material and methods

2.1. Cultivation of *M.aeruginosa*

Cyanobacterium *Microcystis aeruginosa* (FACHB-905) was obtained from the Freshwater Algae Culture Collection at the Institute of Hydrobiology, Chinese Academy of Sciences, China. Axenic cultures were grown in 800 mL photo-bioreactors with BG-11 medium (Table S1) under controlled conditions: constant 28 °C, continuous illumination (50 μmol m⁻²·s⁻¹), and filtered air enriched with 3 % (v/v) CO₂ for carbon supply and hydrodynamic mixing. Algal cells harvested on day 15 of the logarithmic growth phase were utilized for subsequent experiments. By this time, the algal cell count had already reached the threshold indicative of a severe bloom, thereby meeting the experimental requirements (Lui et al., 2011; Nie et al., 2023). The growth curve of algal cells is shown in Fig. S1.

2.2. Separation of algal cells and AOM

The cyanobacterial cells and AOM were separated by centrifugation (4000 rpm, 10 min) using Allegra X-15R Centrifuge (Beckman Coulter, USA) (Qu et al., 2012). The supernatant was filtered through a 0.45-μm membrane to isolate AOM, and the pelleted cells were washed three times with distilled water to obtain AOM-free biomass. The pH of the pure water used for the preparation and washing of algae cells was adjusted to 8, which is the pH of the original culture liquid.

2.3. Coagulation-flotation experiment

The coagulation-flotation experiments were carried out using a convenient coagulation jar tester (TA6, Meiyu, China) equipped with six custom 250 mL glass beakers and a dissolved air system (GWNB1, Gongyuan, China) for micro-bubble generation. The original algal solution was diluted with pure water adjusted to a pH of 8 to achieve a concentration of 2 × 10⁷ cells·mL⁻¹, while the concentration of AOM was measured at 19.74 mg·L⁻¹. This concentration was selected because it represents the established threshold density indicative of severe algal bloom conditions, thereby effectively simulating high-algae scenarios during actual bloom events. Critically, the generated AOM level (19.74 mg L⁻¹) aligns with that reported in a relevant study (Cheng et al., 2022), which demonstrates that elevated AOM concentrations exceeding 10.71 mg L⁻¹ significantly inhibit coagulation efficiency for algae removal. Aluminium sulfate was chosen as the coagulant and purchased from China National Pharmaceutical Group Chemical Reagent. The coagulant stock solution was prepared at a concentration of 10 g·L⁻¹ Al³⁺. In order to investigate the effect of pH on the efficiency of coagulation-flotation for algae removal, the coagulation-flotation efficiency of the original algal solution (pH = 8) and the acidified algal solution (pH = 5 and pH = 2) under different Al³⁺ dosages were compared. A volume of 200 ml of the original algal suspension or acidified algal suspension was adjusted to pH 6.5 after the addition of the predetermined concentration of coagulant for coagulation experiments. The rapid pH adjustment of algal cultures was achieved using an automatic titrator (Titrand 907, Metrohm, Switzerland) equipped with a pH probe. The target pH was set via the instrument's integrated Tiamo software, while the magnetic stirrer was maintained at a constant rotation speed of 50 rpm. The system automatically dispensed pre-prepared 1 M HCl or 1 M NaOH to achieve precise and rapid pH modulation, with the entire process typically completed within 30 s.

The coagulation experiment involved rapid stirring (300 rpm) for 50

s, followed by slow stirring (50 rpm) for 5 min (Li et al., 2022). Subsequently, 50 ml of micro-bubble water was introduced, and the mixture was allowed to settle for 5 min. A dosage determined based on established literature (Cheng et al., 2024) indicating that effective micro-bubble addition for separation processes typically constitutes 20–30 % of the total volume. To ensure representative conditions, we adopted the median value of this range (25 %). Given the total working volume of 200 mL, the calculated requirement was precisely 50 mL (200 mL × 25 %). A 10 ml aliquot of the supernatant was collected and the sample's absorbance at 680 nm was measured using a UV-visible spectrophotometer (VA23230, HACA, USA). The removal efficiency was then calculated using the following formula:

$$\text{Removal efficiency} = (OD_b - OD_a \times 1.25) \times 100\% / OD_b \quad (1)$$

Where OD_b and OD_a represent the absorbance of algal solution before and after coagulation-flotation, respectively. Furthermore, under the condition of controlling the number of algal cells and AOM concentration, the coagulation-flotation efficiency of different combinations of algal cells, acidified algal cells with AOM, and acidified AOM was compared to investigate the respective impacts of algal cells and AOM on coagulation-flotation. The coagulation-flotation tests of the pre-oxidation algal solution with potassium permanganate and ozone were carried out.

2.4. Chlorination experiment and DBPs analysis

Experimental groups demonstrating algal removal efficiencies exceeding 90 % through individual coagulation, acid-enhanced coagulation, and pre-oxidation enhanced coagulation with dissolved air flotation were selected for further analysis. A 50 mL volume of the supernatant was taken, and sodium hypochlorite was added at a concentration of 10 mg·L⁻¹ to initiate the chlorination disinfection process. The extraction of DBPs was conducted utilizing the methyl tert-butyl ether (MTBE) liquid-liquid extraction technique (Wang et al., 2020). Subsequent to the extraction process, the concentrations of specific DBPs: trichloromethane (TCM), bromodichloromethane (BDCM), dichloroacetonitrile (DCAN), trichloroacetonitrile (TCAN), dichloroacetic acid (DCAA), and trichloroacetic acid (TCAA). The quantification of these analytes was performed using gas chromatography equipped with an electron capture detector (Peng et al., 2023) (Agilent 7890, Santa Clara, USA).

2.5. Characterization of algal cells and AOM

2.5.1. Algal cell integrity assessment

The integrity of algal cells was determined using a flow cytometer (Beckman, CytoFlex, USA). Following centrifugation (4000 rpm, 10 min), algal cells were resuspended in PBS phosphate buffer. Subsequently, 20 µM SYTOX dye (KGA261, Kaiji Biology, China) was added to the samples, which were then incubated in the dark at room temperature for 20 min. After incubation, algal cells were resuspended again in PBS phosphate buffer, and fluorescence intensity was measured and analyzed using a flow cytometer (Roth et al., 1997). Algal cells were excited with a 488 nm argon laser, and 10,000 cells were collected for each sample. The data were represented as the percentage of cells that had been stained with SYTOX dye.

2.5.2. Dissolved organic carbon (DOC), charge density, zeta potential, and functional groups

The DOC of AOM was quantified using a total organic carbon analyzer (GmbH, Elementar, Germany). The charge density of AOM was measured by titration with standard positive and negative charge solutions (cationic poly-electrolyte: 0.001 eq·L⁻¹ polyDADMAC, anionic poly-electrolyte: 0.001 eq·L⁻¹ polyPVS-Na) using a charge analyzer (CCA3100, Chemtrac, USA) (Kam and Gregory, 1999). The zeta potential of algae cells and AOM was quantitatively measured using a Zeta

potential analyzer (ZEN 2600, Malvern, UK) (Roth et al., 1997; Wang et al., 2021). The protonated functional groups of algae cells and AOM were titrated with 0.1 M HCl using an automatic potentiometric titrator (Metrohm 907, Metrohm, Switzerland) (Cheng et al., 2022; Naceradska et al., 2019a).

2.5.3. Analysis of molecular weight distribution

The molecular weight distribution of AOM was analyzed using a high-performance liquid chromatography system (1260, Agilent Technologies, USA) coupled with a UV detector (Waters 1260, Waters, USA) by the gel permeation chromatography (GPC) (Zhang et al., 2021). The molecular weight ranges (>100 kDa, 1–100 kDa, <1 kDa) were determined based on retention time, and the proportion of each molecular weight was calculated by integrating the area under the curve.

2.5.4. Protein and polysaccharide content and fluorescence characteristics

The proteins and polysaccharides in AOM were quantified using modified Bradford micro-assay method (López et al., 1993) and the phenol-sulfuric acid method, respectively. The fluorescence components of AOM were characterized using the excitation-emission matrix method (F-2700, Hitachi High-Tech Group, Japan) (Guan et al., 2014; Sha et al., 2019). The operational parameters were set as follows: the excitation wavelength was incrementally scanned from 220 nm to 450 nm with a step size of 5 nm, and the emission wavelength was incrementally scanned from 250 nm to 600 nm with a step size of 2 nm. The PMT voltage was set at 700 V, and distilled water was used as a blank for zero calibration during the measurements.

2.5.5. FT-ICR-MS analysis

The analysis of molecular structural composition is conducted using Fourier Transform Ion Cyclotron Resonance Mass Spectrometry (FT-ICR-MS) (Solarix 15T, Bruker, America). The following formulas are obtained from the aforementioned samples obtained from FT-ICR-MS in order to describe the variations during acidification of AOM (Raeke et al., 2016). The primary detection parameters are as follows: the injection mode is continuous, with an injection rate of 120 µL/h; the capillary inlet voltage is set at 4 kV; the ion accumulation time is 0.06 s; the mass range for acquisition is 100–1600 Da; and the time-domain signal is overlaid 300 times to enhance the signal-to-noise ratio. Prior to sample detection, the instrument is calibrated with 10 mmol/L sodium formate, and after sample detection, internal calibration is performed using soluble organic matter with known molecular formulas. After calibration, the mass accuracy of detection is less than 1 ppm.

2.5.6. SEM analysis

Scanning electron microscopy (SEM) (S4800, Hitachi, Japan) was therefore used to observe morphology variation of AOM. The test parameters include an acceleration voltage of 3.0 kV, a working distance of 1 mm, and a magnification of 10,000 times.

2.6. Statistical analysis

All the experiments were conducted with three biological replicates to ensure the accuracy of the results. The average value (MEAN) and standard deviation (SD) from three duplicate experiments were calculated and used for discussion in this study. All graphs of this study were generated using Origin 2024. 3D-EEM data was analyzed using Matlab to subtract the background values, and resulting fluorescence spectra were plotted using Origin2024.

3. Results and discussions

3.1. Performance of a novel acidified enhanced coagulation process for cyanobacteria removal

The process of algae coagulation typically involves the addition of a

coagulant (aluminum sulfate, Al^{3+}) to algae-laden water, followed by adjusting the pH to the optimum pH of around 6.5. This is followed by rapid and slow stirring to coagulate the algal cells and form flocs. As shown in Fig. 1a, this conventional method of algal coagulation requires 15 mg L^{-1} of Al^{3+} to achieve a removal efficiency of over 90 % by coagulation-flotation. In contrast, we propose a new algal coagulation method. Before adding the coagulant, the pH of the algae-laden water is adjusted to 5 using acid. Subsequently, based on experimental comparisons, we selected a 1-min acidification step for coagulant addition (Fig. 1b), as studies demonstrated that this duration was sufficient to achieve the desired coagulation enhancement effect. Shorter durations (30 s) were potentially inadequate to produce consistent results, and since significant enhancement was already attained at 1 min, longer durations (2 min) were deemed unnecessary. After acidifying the algae-containing water for 1 min, the pH is immediately readjusted back to 6.5 prior to adding the coagulant to initiate the coagulation process. A comparative analysis was conducted to evaluate the acidification-enhanced coagulation efficiency of algal cells at different pH levels (2, 4, and 5) with varying coagulant dosages (Fig. S2). The results demonstrate that when the coagulation efficiency exceeds 90 % (i.e., coagulant dosage $>4 \text{ mg L}^{-1}$), the coagulation enhancement effects of these three target pH levels on algal cells are comparable. Notably, the coagulation efficiencies of acidified algal cells at these pH levels were significantly higher than those of non-acidified controls. In this study, pH 2 and 5 were employed to represent strong and mild acidification conditions, respectively (Naceradska et al., 2019b). Surprisingly, the mild acidification at pH 5 also exhibited substantial enhancement of coagulation efficiency. However, considering the reagent cost and ionic strength

implications in actual water treatment processes (Table S2), pH = 5 was selected as the optimal condition. This choice is further supported by BG11's inherent buffering capacity (primarily from phosphate and carbonate systems), which minimizes acid consumption during pH adjustment. Critically, at pH = 5, the combined ionic strength contribution from added H^+ and Cl^- ions is only 10^{-5} M , which is negligible compared to BG11's baseline ionic strength of 0.0206 M . Meanwhile, results indicate that acidified enhanced coagulation also effectively improved the removal efficiency of *Pseudanabaena* sp. (Fig. S6). This acidification treatment of algae-laden water therefore significantly enhances the efficiency of the removal of algae by coagulation-flotation.

In the acidification treatment, the coagulation improvement is achieved within only 1 min (Fig. 1b). Interestingly, the final coagulation-flotation removal efficiency is also affected by the timing of coagulant addition during the acidification treatment. The optimum order of addition is the one described above. Another approach is to acidify the algae-laden water and then adjust the pH back to the original pH of the algal containing water prior to the addition of the coagulant. Although this approach achieves a higher final coagulation removal rate than the conventional method, and can increase the coagulant flotation removal efficiency from the conventional 35 %–75 % by extending the acidification to 5 min, it is still not as effective as the conventional acidification coagulation method in terms of coagulation-flotation removal rate. This suggests that before the addition of the coagulant, there is a change in the properties of algal cells or AOM before coagulant addition, and this change enhances the interaction between the coagulant and algal cells. However, this change is attenuated and the effect of acidification-induced coagulation is less pronounced when the pH is readjusted.

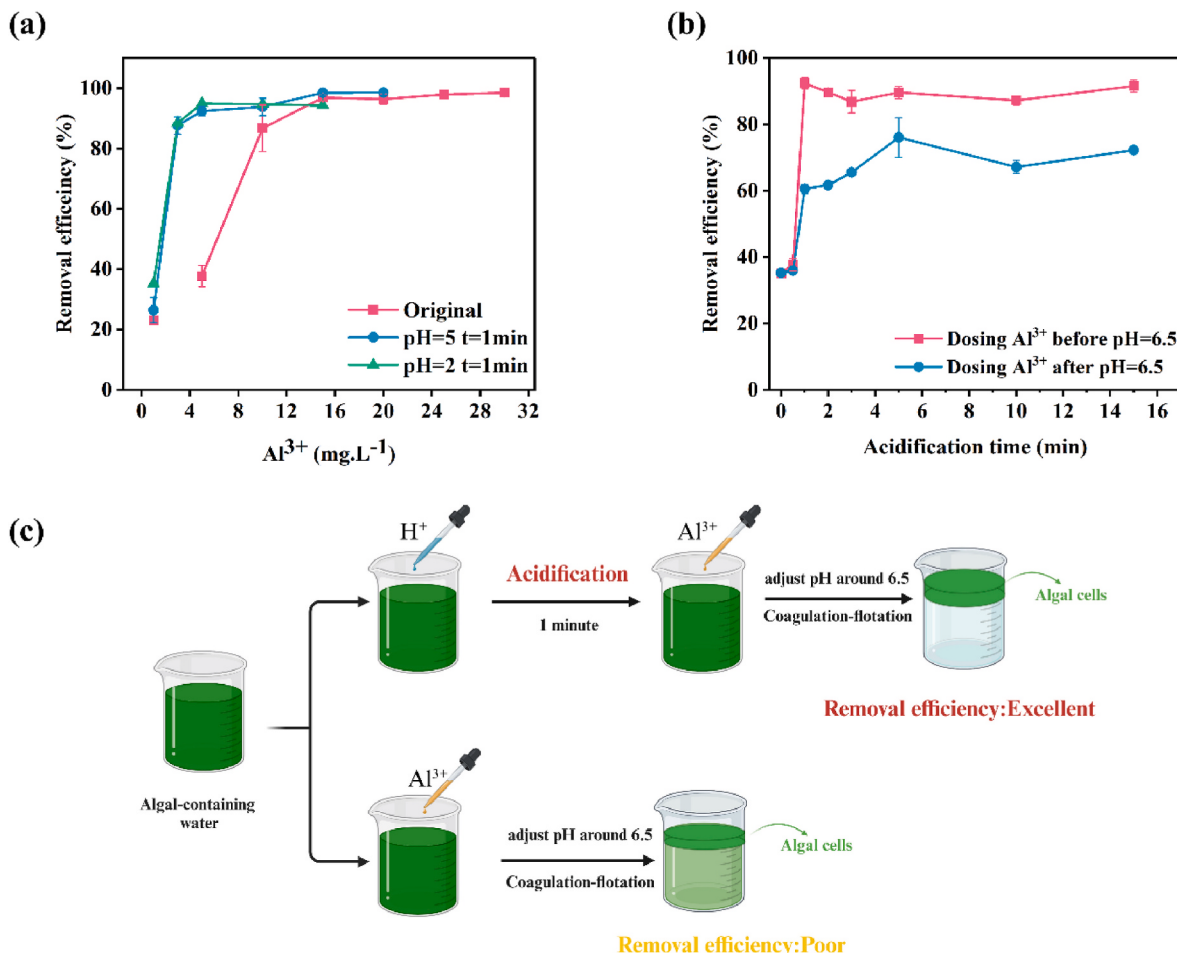


Fig. 1. Comparison of the removal efficiency between acidified algal cells and untreated algal cells (a) and effect of acidification time and coagulant addition order on the removal efficiency of algal cells (b); and experimental protocol sequence for acidification-enhanced coagulation (c).

Thus, it is clear that this acidification step needs to be completed prior to adding coagulant in order to achieve the desired enhanced coagulation of the algal cells (Fig. 1c).

3.2. Algae or AOM reaction enables acidification process to improve coagulation

The conclusions drawn from the previous sections highlight that acidifying algae-laden water significantly decreases DOC without affecting the algae cells themselves, unlike conventional pre-oxidation processes. Reciprocal validation experiments show that while algal cell acidification alone has a negligible effect on coagulation, AOM acidification is the main contributor to enhanced coagulation, as shown in Fig. 2a. Specifically, when only AOM is acidified, a substantial improvement in the coagulation efficiency is observed, whereas the acidification of algal cells does not have a similar effect. This selective reduction of the AOM content during the acidification process, which changes its composition without damaging the algal cells, has a direct effect on improving coagulation. This is in contrast to conventional pre-oxidation methods, which affect both algae cells and AOM, often leading to algae cell rupture and AOM release. Thus, acidification selectively targets AOM and strengthens coagulation without damaging the algae, which is a more cell-friendly approach, with the added benefit of minimized DBPs formation.

It can be posited that the process of acidification has a significant effect on the coagulation process, and this can be explained by examining the compositional alterations within AOM. Fig. 2b illustrates that there is a substantial decrease in the concentration of proteins and polysaccharides, of over 50 %. Specifically, there is a decrease in protein concentration from 2.44 mg L^{-1} to 1.12 mg L^{-1} , while the concentration

of polysaccharides drops from 5.92 mg L^{-1} to 2.86 mg L^{-1} . The reduction in macromolecular content is visually corroborated during the acidification process. Notably, substantial material retention was observed upon filtration of acidified AOM (AAOM) through a $0.45\text{-}\mu\text{m}$ membrane, a phenomenon not exhibited by non-acidified AOM (Fig. S3). These observations suggest that the acidification process results in the precipitation of certain AOM components, thereby reducing their solubility and their ability to impede coagulation.

Specifically, the FRI analysis revealed a significant decrease in the relative fluorescence intensity of aromatic protein-like compounds within AOM, with the intensity decreasing by 40.37 % (Table S3). In contrast, fulvic acid-like and humic acid-like substances exhibit no significant changes (Fig. 2c and d). The present findings lend further support to the hypothesis that the reduction in protein-like compounds, which are known to interfere with coagulation, plays a pivotal role in the enhanced coagulation observed after acidification. It has previously been established that AOM, particularly proteins and anionic polysaccharides, can impede algae flocculation by binding with coagulants, thereby increasing coagulant demand (Roselet et al., 2017; Vandamme et al., 2016). The reduction of these inhibitory macromolecules following acidification provides a clear explanation for the enhanced coagulation effect, as the decreased protein and polysaccharide content in AOM allows coagulants to interact more effectively with algal cells, facilitating their removal.

3.3. Mechanism of enhanced coagulation with the novel acidification

3.3.1. Elucidation of mechanism from composition and molecular perspectives

The primary components removed from AOM, exhibiting higher

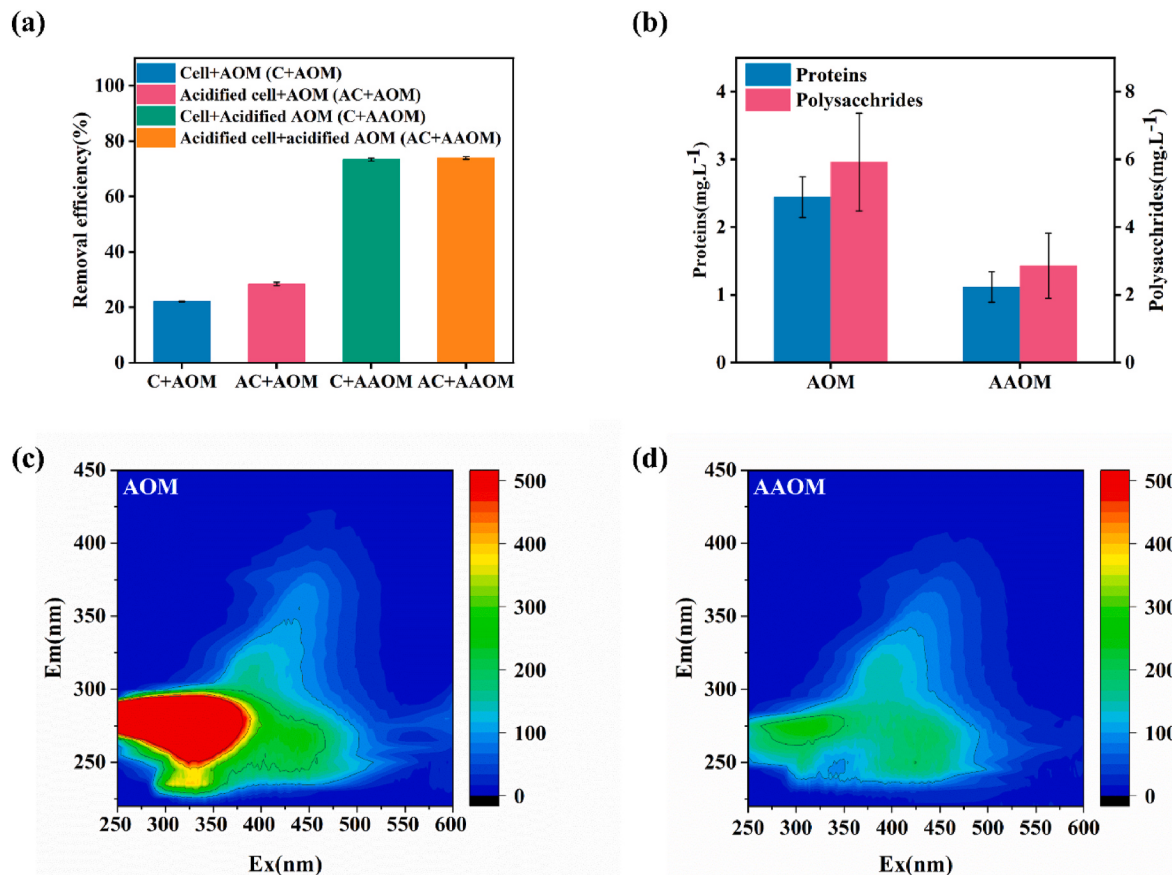


Fig. 2. Comparison of the removal efficiency of algal solution with the combination of the unacidified and acidified cells (AC) or acidified AOM (AAOM) (a), protein and polysaccharide composition (b), fluorescence components (c and d).

intensities, are carbohydrates and proteins (Ruan et al., 2021). As illustrated in Fig. 3a, the size of each data point is proportionate to its intensity. Post-acidification, the carbohydrates and proteins underwent a significant decrease of 16.7 % and 23.2 % respectively (Table S4), as illustrated in Fig. 3b. This finding suggests that the molecules responsible for the inhibition of coagulation, namely proteins and polysaccharides, underwent a reduction following the acidification process. These results are consistent with previous findings, which indicated that there was a reduction in the DOC concentration and a decrease in

fluorescence peaks associated with protein-like substances. The apparent discrepancy between the substantial reduction (>50 %) in protein and polysaccharide concentrations measured by conventional assays (Fig. 2b) and the more modest reductions observed via FT-ICR-MS arises from fundamental differences in the analytical techniques. FT-ICR-MS excels at molecular-level characterization but primarily detects compounds below 1500 Da (Cao et al., 2015) and is notably susceptible to fragmentation of larger biomolecules during electrospray ionization (ESI). This fragmentation prevents the direct detection and

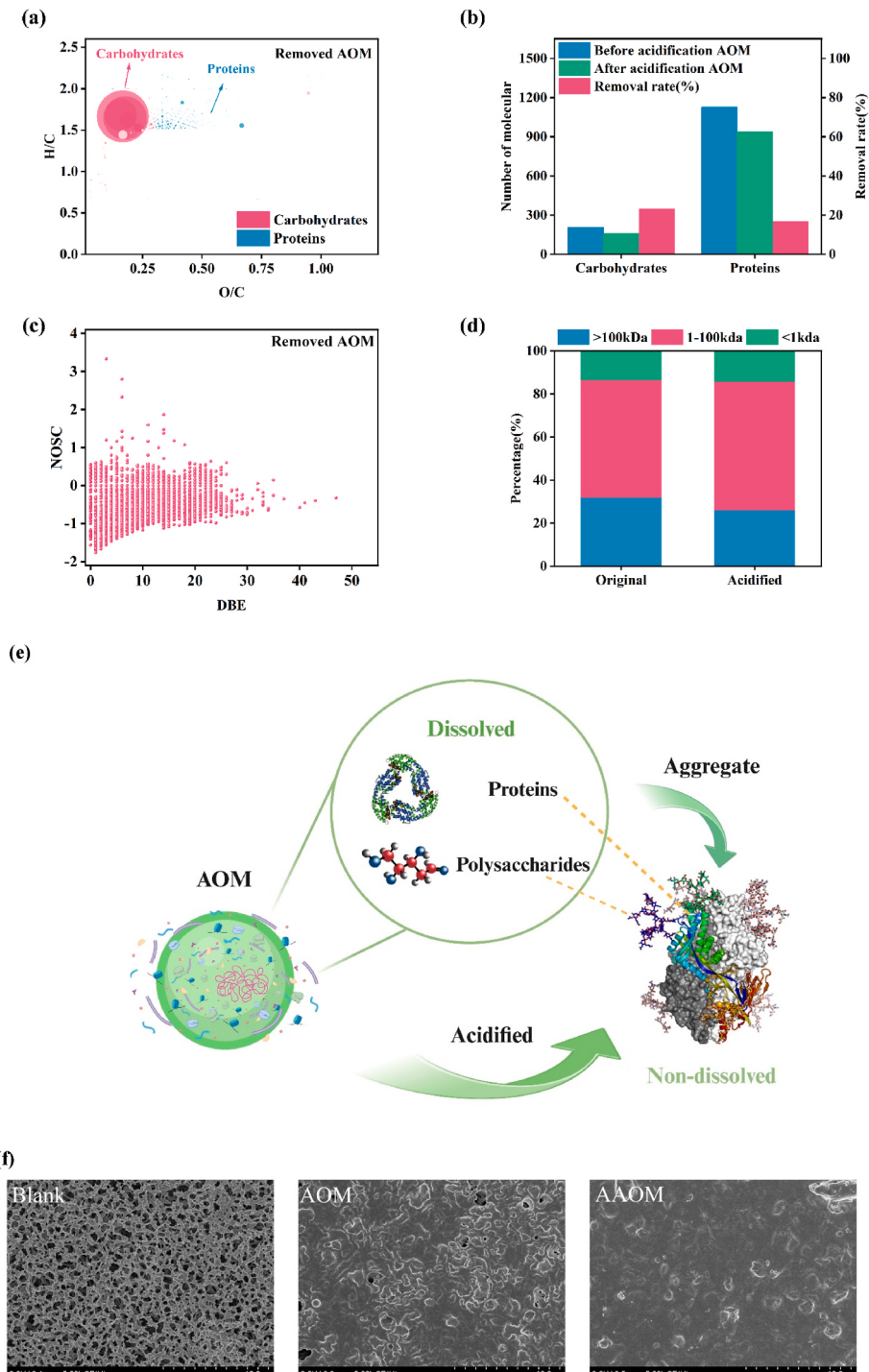


Fig. 3. Characterization of AOM removal and transformation post-acidification: (a) Van Krevelen diagram of AOM removal, (b) molecular formula variations, (c) polarity of removed AOM molecules, (d) molecular weight distributions, (e) precipitation of macromolecules, and (f) SEM images demonstrating substantially greater material deposition exclusively on membranes filtered with acidified AOM compared to non-acidified AOM and blank controls.

quantification of intact large proteins and polysaccharides, masking their true abundance and loss. In contrast, the conventional phenol-sulfuric acid and modified Bradford micro-assay methods target specific functional groups indicative of polysaccharides and proteins, respectively, and are sensitive to intact macromolecules across a broad size range. Consequently, the >50 % reduction measured conventionally reflects a significant loss of functional macromolecular protein and polysaccharide structures due to acidification. The smaller reductions observed by FT-ICR-MS primarily represent changes within the low molecular weight fraction (<1500 Da) and potentially include new fragments generated from the breakdown of larger molecules; thus, FT-ICR-MS inherently underestimates the true extent of macromolecular removal. This difference underscores that the techniques provide complementary perspectives: the biochemical assays quantify the loss of functional macromolecules, while FT-ICR-MS reveals compositional shifts primarily within the lower molecular weight pool and fragmentation products.

To further investigate the mechanisms of acidification, an approach known as the nominal oxidation state of carbon (NOSC) was employed, as this represents a means to indirectly reflect the polarity of molecules (Cao et al., 2015). As shown in Fig. 3c, the molecules that decreased following acidification treatment are positioned near the lower-left corner of the graph, suggesting that the acidification process preferentially removes components of AOM that are typically less polar and which are also known to exhibit poor water solubility. GPC analysis revealed that the proportion of substances with molecular weights exceeding 100 kDa in AAOM decreased significantly compared to the original AOM, from 31.8 % to 26.0 % (Fig. 3d). This marked reduction in large-molecule components such as proteins and polysaccharides might serve as a prerequisite for the enhanced coagulation of algal cells through acidification.

The results obtained demonstrate unequivocally that the molecules removed during the process of acidification are characterized by reduced polarity, lower aqueous solubility, and larger molecular size. The synergistic effects ultimately induced a marked reduction in solubility for specific protein and polysaccharide components within the acidified AOM, leading to their precipitation and phase transition from soluble to insoluble forms, as evidenced by the present study (Fig. 3e). Direct evidence of this retention mechanism is provided by SEM imaging (Yu et al., 2024): comparative analysis of membranes filtered with equal volumes of non-acidified AOM, acidified AOM (AAOM), and blank controls revealed substantially greater material deposition exclusively on AAOM-treated membranes (Fig. 3f). The phenomenon was corroborated by significant membrane fouling during filtration of AAOM, as evidenced by substantial accumulations of retentate on the membrane surface (Fig. S3). Alterations of pH result in complexation reactions and precipitation of the aforementioned molecules out of solution (Guo et al., 2020; Li et al., 2023). The pH of proteins falls below their isoelectric point (PI), causing them to gain a net positive charge, while the negative charge of polysaccharides typically remains. The net positive charge acquired by proteins, as opposed to the predominantly negative charge of polysaccharides, serves to augment electrostatic attraction between these macromolecules, thereby facilitating complexation. The present study observed that alterations in pH induce the formation of protein-polysaccharide complexes, which subsequently precipitate out of the solution, thus validating the prevailing notion that the modulation of charges driven by pH underpins these interactions. Consequently, these complexes relinquish their occupancy of the binding sites for coagulants, thereby enabling algal cells to engage preferentially with the coagulants. This, in turn, enhances the efficiency of the coagulation process, leading to improved removal of algal cells. These observations offer novel insights into the manner through which the process of acidification impacts the solubility of AOM components.

3.3.2. Elucidation of mechanism from molecular interaction perspectives

The present study investigates the impact of acidification on algae-

laden water, with a particular focus on the alterations in compositional characteristics of AOM. The results reveal a significant reduction in macromolecular constituents, including proteins and polysaccharides. Structural alterations in acidified AOM are hypothesized to predominantly contribute to enhanced coagulation efficiency of algal cells, with minimal effect on cellular integrity. The study revealed that proteinaceous substances and acidic polysaccharides within AOM preferentially interact with coagulants through specific electrochemical mechanisms, resulting in significantly increases in coagulant consumption and subsequent reductions in availability to algal cells. It is hypothesized that the underlying mechanism of this increased coagulant consumption is predominantly attributed to the electrostatic interactions between negatively charged functional groups (e.g., carboxyl groups) present on these AOM constituents and the positively charged sites on the coagulant molecules (Cheng et al., 2022; Quang Viet et al., 2019; Zang et al., 2020). As expected, the negative zeta potential of the system containing acidified algae exhibited a substantial reduction, decreasing from -28.73 to -25.38 mV (Fig. 4a). The findings reveal that acidification, when used as a standalone agent, yielded a zeta potential modification that exhibited comparable efficacy to that achieved with the addition of 10 mg L⁻¹ of Al³⁺ coagulant. This observation signifies a fundamental modification in charge distribution within the solution environment, induced by alterations in the composition of AOM, caused by acidification.

Conventional coagulation mechanisms propose that positively charged hydrolysates from metal salt coagulants enhance algal cell aggregation through two primary pathways: double layer compression and charge neutralization. This is thought to be effective in reducing the electrostatic repulsion between negatively charged algal cells, thereby facilitating floc formation (Ai et al., 2020; Kong et al., 2021). This mechanism is consistent with the observations of flocculation in non-acidified, algae-laden water containing Al³⁺ coagulant. However, despite the significant reduction in zeta potential, no spontaneous flocculation of algal cells was observed in acidified algae-laden water prior to coagulant addition, nor was there an additional zeta potential reduction with the introduction of 5 mg L⁻¹ coagulant to the acidified system. These findings collectively indicate that the enhanced coagulation performance in acidified systems cannot be solely attributed to the conventional mechanisms of reduced intercellular repulsion. Rather than being attributable only to the conventional mechanisms of reduced intercellular repulsion, these results suggest the existence of alternative, potentially synergistic mechanisms which may contribute to improved algal cell coagulation efficiency. As illustrated in Fig. 4b, AAOM exhibited a substantial reduction in negative charge density compared to its native counterpart. Additionally, an approximate 50 % decrease in negatively charged carboxyl functional groups was observed within AAOM. However, the carboxyl group content of acidified algal cells remained virtually unchanged (Fig. 4c). This compelling evidence suggests that the enhanced coagulation is predominantly attributable to the acidification-induced modifications in AOM's charge characteristics and functional group composition, rather than alterations to the algal cells themselves.

A comprehensive analysis was performed on acidification-induced modifications in AOM, encompassing alterations in material composition, charge, and functional group, to reveals a multi-faceted enhancement mechanism. The introduction of excess hydrogen ions during acidification has been shown to interact preferentially with negatively charged functional groups (e.g., carboxylate groups) in AOM, leading to their protonation and potential approach to the isoelectric point of proteinaceous substances (Ai et al., 2020; Liu et al., 2022; Wang et al., 2018). The process of protonation can effectively reduce inter-molecular repulsion forces, facilitating molecular aggregation and complexation. The outcome of these processes is the formation of larger molecular structures which can transition into insoluble colloidal forms (as evidenced by membrane retentate analysis) (Jones and O'Melia, 2000). These transformations yield dual benefits. Firstly, it has been shown that

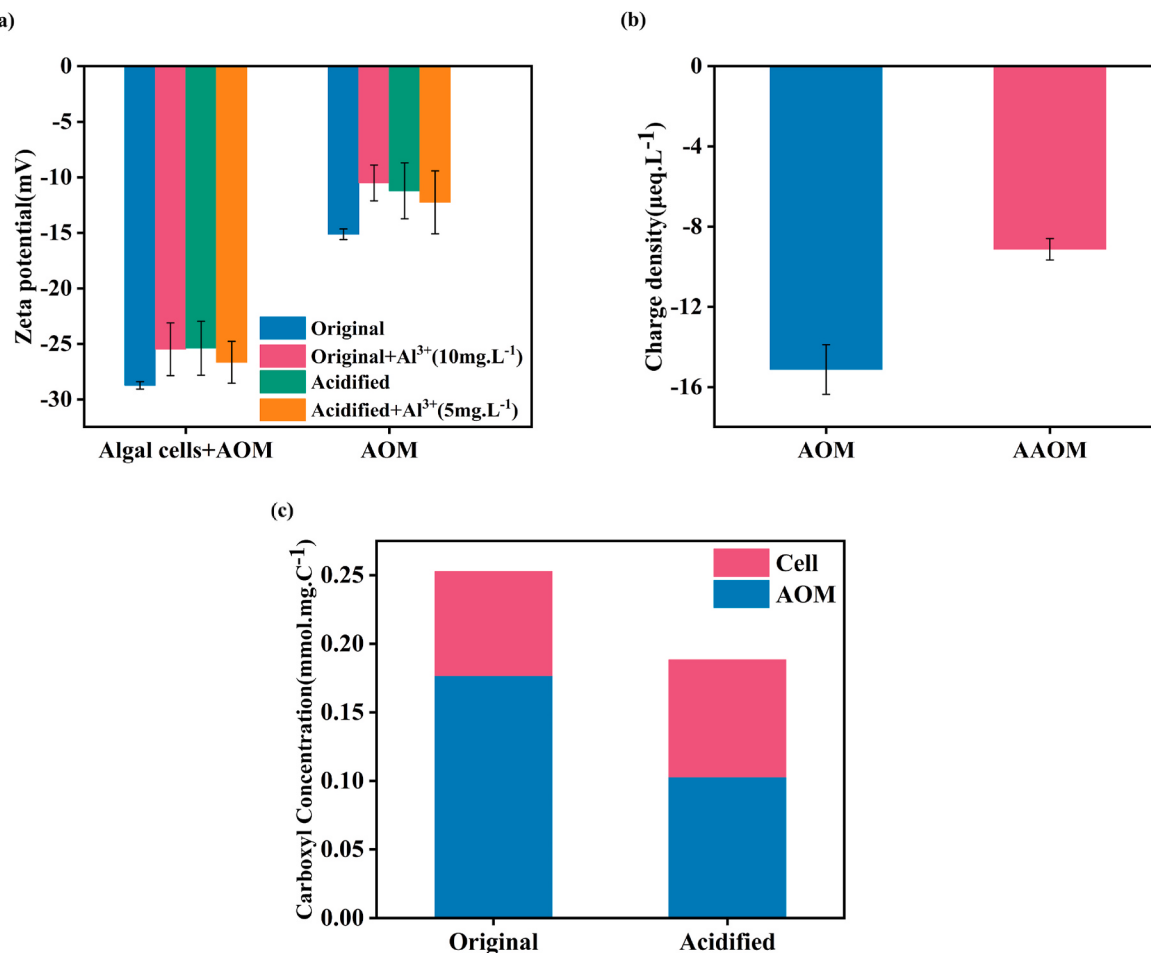


Fig. 4. Comparison of zeta potential (a), charge density (b) and carboxyl groups (c) following acidification.

removing AOM components before coagulation increases the probability of coagulant-algal cell interactions (Cheng et al., 2024; Lama et al., 2024); secondly, complex macromolecular colloids in AAOM can

enhance coagulation efficiency by improving sweep flocculation and entrapment mechanisms (Cai et al., 2021). These effects work together to greatly improve the coagulation performance of algal cells.

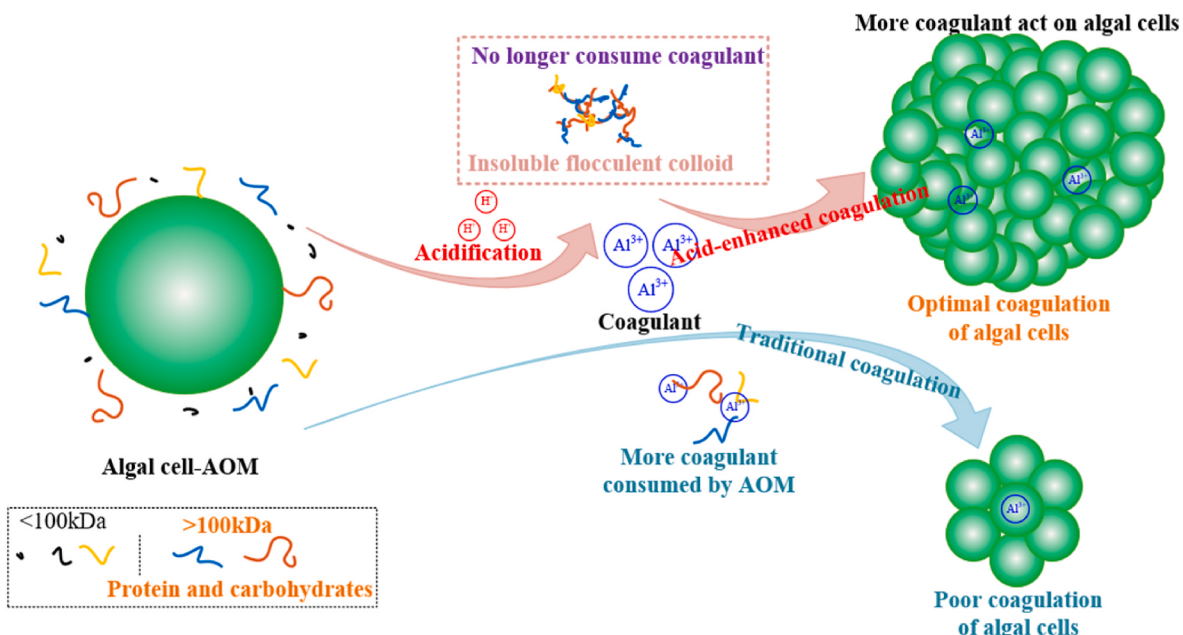


Fig. 5. The mechanistic insights into acid-mediated enhancement of coagulation in algal cell aggregation.

3.3.3. Mechanism of acidification-enhanced coagulation for algal removal

The combined effects of acidification on AOM components, including macromolecule reduction (proteins/polysaccharides), physicochemical property alterations (polarity, zeta potential, charge density), and chemical composition changes (carboxyl group concentrations), collectively elucidate the fundamental mechanism driving improved algal cell coagulation in algae-laden water systems. Acidification has been shown to selectively target AOM, leading to the preferential reduction of macromolecular substances that are rich in negatively charged functional groups, such as carboxyl groups (Henderson et al., 2008; Yang et al., 2018). These macromolecules, due to their charge distribution, would otherwise interact with coagulants, occupying the positively charged sites. This, in turn, impedes the coagulant-algal cell interaction, thereby inhibiting the coagulation process (Ma et al., 2022; Zang et al., 2020). This inhibitory effect is thereby weakened or eliminated, facilitating the enhanced coagulation of algal cells.

As demonstrated in Fig. 5, the mechanism of acidification-induced coagulation enhancement highlights the pivotal role of AOM in this process, as opposed to the algal cells themselves. The aggregation of high molecular weight components, such as proteins and polysaccharides, is induced by acidification through reducing electrostatic repulsion and driving them towards their isoelectric points. This aggregation process leads to the formation of visible flocculent colloidal substances, which undergo a transition from a dissolved to a non-dissolved state. This transition is accompanied by a significant reduction in the negative charge density of carboxyl groups (-COO⁻) within AOM. Furthermore, the aggregation process results in the formation of network-like complexes, which are comprised of proteins and polysaccharides (Cai et al., 2021). These complexes serve to enhance the network trapping effect, thereby promoting the coagulation process. SEM observations (Fig. 3f) have visually confirmed the presence of such network structures formed by AOM aggregates under acidified conditions. To quantitatively assess the impact of acidification on the floc characteristics, the size distribution of flocs formed during the coagulation process (with and without prior acidification) was analyzed using our previously established floc photography system (Cheng et al., 2025) (Fig. S4). As shown in Fig. S5, flocs formed under acidified conditions exhibited a significantly larger average size compared to those formed by direct coagulation without acidification. This increase in floc size is consistent with the formation of the more extensive network-like complexes observed by SEM and provides direct evidence supporting the enhanced entrapment capability attributed to these structures. The interplay of these dual mechanisms – the reduction of electronegative substances and sweep coagulation – functions synergistically, thereby enhancing the removal efficiency of algal cells from the water. This, in turn, establishes an environment conducive to the enhanced interaction of coagulants with algal cells, thus leading to an augmentation in coagulation efficiency.

Contrary to conventional pre-oxidation that directly damages algal cells and releases IOM, the proposed AEC strategy employs pH 5-controlled interfacial protonation to selectively aggregate proteins and polysaccharides in AOM, while preserving cell integrity. This dual mechanism—selective AOM removal coupled with cell protection—not only minimizes IOM release and subsequent DOC elevation, but under optimal conditions achieves 60 % coagulant saving and 30 % reduction in DBPs formation, thereby achieving synergistic optimization of process efficacy and chemical risk control in algal bloom control. The efficacy of this method is further substantiated by successful coagulation trials employing PAC or PAM as coagulants, as detailed in Table S5 and Fig. S8. In addition, coagulation experiments conducted with polyacrylamide (PAM) as the coagulant revealed that acidification enhances coagulation effectiveness without altering the coagulant's morphology, thereby corroborating the earlier assertion that acidification exerts its influence on AOM. Collectively, this study demonstrates an innovative strategy for optimizing algal coagulation in drinking water treatment, effectively mitigating the drawbacks inherent to conventional

approaches.

3.4. Benefits of acidification compared to pre-oxidation

A non-pre-oxidative treatment for algal coagulation can be considered as acidification-enhanced algal cell coagulation. As shown in Fig. 6a, the coagulation-flootation efficiency of untreated, acid-treated and separately pre-oxidized algal cells was compared using potassium permanganate (KMnO₄) and ozone (O₃). Compared to 4 mg L⁻¹ KMnO₄ or 2 mg L⁻¹ O₃ pre-oxidation, a simple acidification treatment of algae-laden water for 1 min at the same coagulant dosage of 10 mg L⁻¹ achieves a higher algal cell coagulation removal efficiency of more than 90 %, while the pre-oxidation only achieves around 80 %. Pre-oxidation only achieves a removal efficiency of 90 % when the coagulant dosage is further increased to 15 mg L⁻¹. This suggests that with a reduced coagulant dosage of only two thirds of the latter, the acidification treatment of algal water can achieve better enhanced coagulation effects than the traditional pre-oxidation treatment.

Dissolved organic matter (DOM) removal is also an important indicator in drinking water treatment (Gilca et al., 2020). This is especially true for algal-rich waters, where AOM is the main DOM and a major precursor of DBPs (Liu et al., 2020). Therefore, as shown in Fig. 6b, the response of AOM before and after pre-treatment and coagulation-flootation was also investigated. DOC can be reduced to 5.41 mg L⁻¹ by acidification treatment, to 6.98 mg L⁻¹ by KMnO₄ pre-oxidation, but to 17.86 mg L⁻¹ by O₃ compared to the initial DOC of 9.87 mg L⁻¹. The change in the amount of AOM due to pre-oxidation is mainly attributed to its oxidizing effect, which can oxidize some organics into small molecules. It can also cause cell rupture, releasing IOM, which leads to an increase in DOC rather than a decrease. Interestingly, acidification pre-treatment can reduce the concentration of DOC. This suggests that the soluble AOM decreases when the algae-laden water is acidified. DOC was further reduced to varying degrees by coagulation-flootation. Compared to the other treatments, the coagulation-flootation treated with acidification had the lowest residual DOC of 2.89 mg L⁻¹. This resulted in an overall DOC removal efficiency of almost 50 %. DOC removal efficiencies were less than 40 % for the untreated and O₃ pre-oxidation samples. In contrast, the KMnO₄ pre-oxidation sample had less than 15 % DOC removal, possibly due to the higher proportion of small molecules after pre-oxidation, which are less efficiently removed by coagulation (Jin et al., 2022).

Pre-oxidative often causes algal cells to rupture, releasing IOM and increasing the risk of forming DBPs (Chen et al., 2023; Zhang et al., 2020). This is further supported by comparing algal cell integrity (Fig. 6c). KMnO₄ pre-oxidation (4 mg L⁻¹) results in an increase in algal cell rupture of approximately 60 %. O₃ pre-oxidation (2 mg L⁻¹) results in an even more significant increase in algal cell rupture of nearly 99 %, contributing to the substantial increase in DOC after treatment. In contrast, a minimal damage to algal cells is caused by the acidification pre-treatment. Further evaluation of the potential to produce DBPs following different pretreatments shows a significant increase of over 30 % in the amount of DBPs produced following both pre-oxidation treatments (Fig. 6d). Particularly, the production of DBPs, specifically trichloroacetic acid (TCAA) (Chen et al., 2024; Dong et al., 2019), which is known for its higher toxicity, increased by more than four times. This might be caused by two reasons. Firstly, pre-oxidation causes severe damage to algal cells, leading to cell lysis and the release of substantial amounts of AOM, thereby significantly increasing the precursor load for DBPs. In contrast, acidification primarily adjusts pH, causing considerably less damage to cell integrity, which limits the total release of AOM at the source. Secondly, pre-oxidation fragments larger organic molecules into smaller compounds, which are key precursors for HAAs. Acidification, however, promotes protonation (H⁺) of carboxyl groups (-COOH) to form -COOH₂⁺. This protonated state reduces the reactivity of the carboxyl group towards electrophilic substitution by chlorine during subsequent disinfection, directly inhibiting the formation

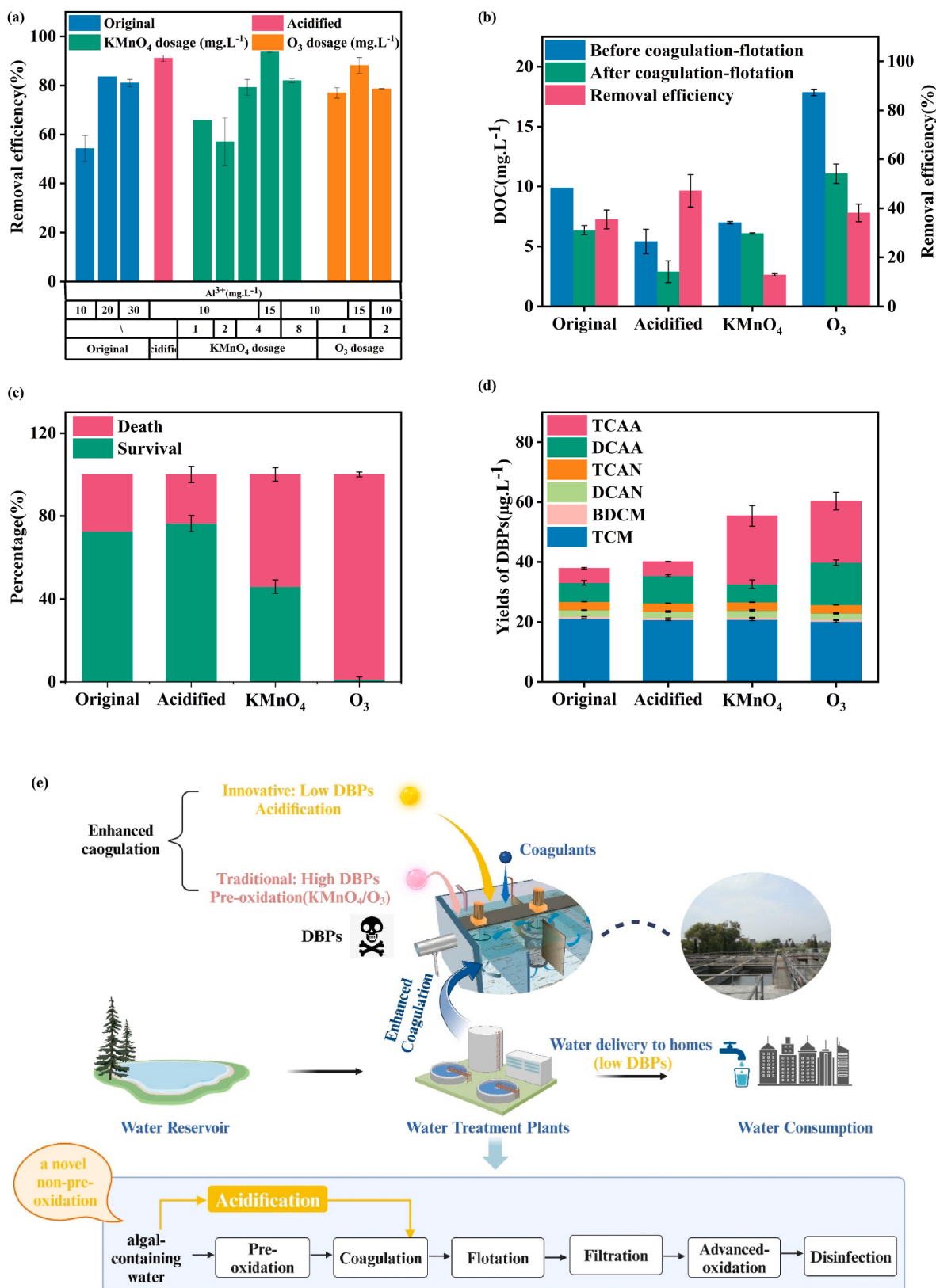


Fig. 6. Comparison of algae removal efficiency of the original, acidified, and pre-oxidized algal suspension (a), AOM extracted from different preprocessed algal solution before and after coagulation-flotation (b), and the cell integrity (c) and the DBPs generation capacity of AOM (d) from differently pretreated algal solutions; and a prospective water treatment methodology, resulting in diminished production of DBPs (e).

pathway of TCAA (Fig. S7).

While pre-oxidation is widely reported to enhance coagulation efficiency and reduce DBPs formation (Qian et al., 2024), the results in Fig. 6d indicate a paradoxical increase in DBPs generation under our experimental conditions. This observation aligns with emerging evidence suggesting that the efficacy of pre-oxidation is strongly dose-dependent. As demonstrated by (Yan et al., 2020), ozone doses of 0.5–4.0 mg.L⁻¹ led to 1.02–1.98 fold increases in THMs compared to non-ozoneated controls, directly linking oxidant overexposure to elevated DBPs yields. Therefore, the risks associated with DBPs from acidification remain lower than those from pre-oxidation. The BG11 medium employed herein (Table S1) established a low-bromide background that significantly influenced DBPs speciation (Guo et al., 2020). THMs analysis revealed detectable BDCM across all treatment processes (0.66–0.68 µg.L⁻¹), whereas TBM and DBCM fell below the detection limit. Crucially, bromide's role in dictating HAA bromination extent is well-established (Chen et al., 2017). Future bromide-gradient experiments will systematically resolve its impact on HAA speciation to advance bromide driven DBPs formation.

Cost is also very important in the actual water treatment process. As both acidification and pre-oxidation processes require equipment such as mechanical stirrers, only reagent costs were considered for treatment expense evaluation. The reagent costs of acidified coagulation, pre-oxidation coagulation, and traditional coagulation were evaluated at a pilot scale of 10 t h⁻¹, as shown in Table 1. The reagent costs per ton of algae-laden water for the three processes were \$0.019, \$0.037, and \$0.053, respectively. Results demonstrate that the acidified enhanced coagulation process reduces economic costs by 64.96 % compared with the traditional coagulation process, while achieving a 49.54 % cost reduction relative to the pre-oxidation coagulation process. Therefore, acid-enhanced coagulation is a promising water treatment process when considering the efficiency of algal cell removal, coagulant dosage, DOC removal capacity, impact on algal cell integrity and the potential for DBPs formation (Fig. 6e).

4. Conclusion

This study proposes a novel acidified method to enhance coagulation for algal removal in drinking water. Results indicate that the algae removal efficiency after brief acidification for 1 min is significantly higher than untreated samples, saving over 60 % of the coagulant. In comparison with traditional pre-oxidation methods, acidification achieves even higher algae removal efficiency, with less damage to cells and a reduction of nearly 30 % in the ability to generate DBPs. During the acidification of algal solution, it is revealed that AOM plays a key role, rather than algal cells. Considering the charge, composition, molecular weight, and functional groups of AOM during the acidification, it is elucidated that the main mechanism of acid-enhanced algal cell coagulation is the aggregation of some large molecules (proteins and polysaccharides) in AOM due to the proximity of pH to the isoelectric point, forming insoluble flocculent colloids that precipitate. Under these effects, substances or functional groups in AOM that inhibit algal cell coagulation decrease, reducing negative electronegativity. This provides the coagulant with more opportunities to interact with algal cells, increasing the efficiency of algal cell coagulation. Meanwhile, the aggregation of macromolecules into network-like complexes enhances the network trapping effect, further strengthening the coagulation process. This multi-faceted reinforcement collectively strengthens the coagulation process. This acidified-enhanced coagulation is also applicable to commonly used coagulants, such as PAC and PAM, in drinking water treatment and proves effective for algae from natural water bodies. This study offers a promising solution to mitigate the formation of DBPs during drinking water treatment, particularly in addressing the rising occurrence of HABs in water sources. It provides a new technological approach to enhance the safety and efficiency of drinking water treatment processes.

Table 1

Reagent cost comparison among acidified coagulation, pre-oxidation coagulation, and traditional coagulation processes.

Treatment	Acidified coagulation	Pre-oxidation coagulation	Traditional coagulation
Reagent type	Industrial-grade hydrochloric acid (33 %)	Potassium permanganate	Aluminum sulfate octadecahydrate
Reagent unit price	28.57	2571.43	142.86
Cost of HCl per ton of water	\$0.010	\	\
Cost of KMnO ₄ per ton of water		\$0.01	\
Cost of Al ₂ (SO ₄) ₃ ·18H ₂ O per ton of water	\$0.009	\$0.027	\$0.053
Total cost per ton	\$0.019	\$0.037	\$0.053

CRediT authorship contribution statement

Xin Chen: Writing – review & editing, Writing – original draft, Methodology, Investigation, Formal analysis, Data curation, Conceptualization. **Yunlu Jia:** Writing – review & editing, Validation, Data curation. **Lili Li:** Validation, Methodology. **Jun Ma:** Writing – review & editing, Validation. **Xuezhi Zhang:** Writing – review & editing, Validation. **Haiyang Zhang:** Writing – review & editing, Writing – original draft, Validation, Methodology, Funding acquisition, Formal analysis.

Statement of informed consent, human/animal rights

No conflicts, informed consent, or human or animal rights are applicable to this study.

Declaration of competing interest

The authors declare no conflict of interests.

Acknowledgements

This research was financially supported by the National Natural Science Foundation of China (42277076), and the Knowledge Innovation Program of Wuhan-Shuguang Project (2023020201020293).

Appendix A. Supplementary data

Supplementary data to this article can be found online at <https://doi.org/10.1016/j.jclepro.2025.146722>.

Data availability

Data will be made available on request.

References

- Ai, Y., Zhao, C., Sun, L., Wang, X., Liang, L., 2020. Coagulation mechanisms of humic acid in metal ions solution under different pH conditions: a molecular dynamics simulation. *Sci. Total Environ.* 702, 135072.
- Cai, Q., Song, K., Tian, C., Wu, X., Li, Y., Huang, Y., Wang, C., Xiao, B., 2021. Harvesting of microcysts from waterbody by flocculation and filtration: the essential role of extracellular organic matters. *J. Water Process Eng.* 41, 102053.
- Cao, D., Huang, H., Hu, M., Cui, L., Geng, F., Rao, Z., Niu, H., Cai, Y., Kang, Y., 2015. Comprehensive characterization of natural organic matter by MALDI- and ESI-fourier transform ion cyclotron resonance mass spectrometry. *Anal. Chim. Acta* 866, 48–58.
- Chen, J., Gao, N., Li, L., Zhu, M., Yang, J., Lu, X., Zhang, Y., 2017. Disinfection by-product formation during chlor(am)ination of algal organic matters (AOM) extracted from *Microcystis aeruginosa*: effect of growth phases, AOM and bromide concentration. *Environ. Sci. Pollut. Control Ser.* 24 (9), 8469–8478.
- Chen, M., Rholl, C.A., Persaud, S.L., Wang, Z., He, Z., Parker, K.M., 2023. Permanganate preoxidation affects the formation of disinfection byproducts from algal organic matter. *Water Res.* 232, 119691.

- Chen, W., Wang, X., Wan, S., Yang, Y., Zhang, Y., Xu, Z., Zhao, J., Mi, C., Zhang, H., 2024. Dichloroacetic acid and trichloroacetic acid as disinfection by-products in drinking water are endocrine-disrupting chemicals. *J. Hazard Mater.* 466, 133035.
- Cheng, S., Zhang, H., Li, L., Yu, T., Wang, Y., Tan, D., Zhang, X., 2022. Harvesting of microcystis flos-aquae using dissolved air flotation: the inhibitory effect of carboxyl groups in ionic acid-containing carbohydrates. *Chemosphere* 300, 134466.
- Cheng, Z., Lin, Z., Chen, X., Zhang, X., Zhang, H., 2025. Unraveling the mechanisms underlying AOM-Induced deterioration of the settling performance of algal floc. *Water Res.* 274, 123115.
- Cheng, S., Zhang, H., Wang, H., Mubashar, M., Li, L., Zhang, X., 2024. Influence of algal organic matter in the in-situ flotation removal of microcystis using positively charged bubbles. *Bioresour. Technol.* 397, 130468.
- Dong, F., Lin, Q., Li, C., He, G., Deng, Y., 2021. Impacts of pre-oxidation on the formation of disinfection byproducts from algal organic matter in subsequent chlor(am)ination: a review. *Sci. Total Environ.* 754, 141955.
- Dong, F., Liu, J., Li, C., Lin, Q., Zhang, T., Zhang, K., Sharma, V.K., 2019. Ferrate(VI) pretreatment and subsequent chlorination of blue-green algae: quantification of disinfection byproducts. *Environ. Int.* 133, 105195.
- Feng, Y., Xiong, Y., Hall-Spencer, J.M., Liu, K., Beardall, J., Gao, K., Ge, J., Xu, J., Gao, G., 2024. Shift in algal blooms from micro- to macroalgae around China with increasing eutrophication and climate change. *Glob. Change Biol.* 30 (1), e17018.
- Gilca, A.F., Teodosiu, C., Fiore, S., Musteret, C.P., 2020. Emerging disinfection byproducts: a review on their occurrence and control in drinking water treatment processes. *Chemosphere* 259, 127476.
- Grzegorzek, M., Wartalska, K., Kazmierczak, B., 2023. Review of water treatment methods with a focus on energy consumption. *Int. Commun. Heat Mass Tran.* 143, 106674.
- Guan, Q., Zheng, H., Zhai, J., Zhao, C., Zheng, X., Tang, X., Chen, W., Sun, Y., 2014. Effect of template on structure and properties of cationic polyacrylamide: characterization and mechanism. *Ind. Eng. Chem. Res.* 53 (14), 5624–5635.
- Guo, L., Fang, Y., Shao, Z., Fang, S., Li, Y., Chen, J., Meng, Y., 2020. pH-induced structural transition during complexation and precipitation of sodium caseinate and ε-Poly-l-lysine. *Int. J. Biol. Macromol.* 154, 644–653.
- He, H.-Y., Qiu, W., Liu, Y.-L., Yu, H.-R., Wang, L., Ma, J., 2021. Effect of ferrate pre-oxidation on algae-laden water ultrafiltration: attenuating membrane fouling and decreasing formation potential of disinfection byproducts. *Water Res.* 190, 116690.
- Henderson, R.K., Baker, A., Parsons, S.A., Jefferson, B., 2008. Characterisation of algalic organic matter extracted from Cyanobacteria, green algae and diatoms. *Water Res.* 42 (13), 3435–3445.
- Hou, X.J., Feng, L., Dai, Y.H., Hu, C.A.M., Gibson, L., Tang, J., Lee, Z.P., Wang, Y., Cai, X. B., Liu, J.G., Zheng, Y., Zheng, C.M., 2022. Global mapping reveals increase in lacustrine algal blooms over the past decade. *Nat. Geosci.* 15, 130–134.
- Jin, Y., Li, P., Xu, B., Wang, L., Ma, G., Chen, S., Tan, F., Shao, Y., Zhang, L., Yang, Z., Chen, F., Li, W., Cheng, X., Wu, D., 2022. A novel technology using iron in a coupled process of moderate preoxidation-hybrid coagulation to remove cyanobacteria in drinking water treatment plants. *J. Clean. Prod.* 342, 130947.
- Jones, K.L., O'Melia, C.R., 2000. Protein and humic acid adsorption onto hydrophilic membrane surfaces: effects of pH and ionic strength. *J. Membr. Sci.* 165 (1), 31–46.
- Kam, S.K., Gregory, J., 1999. Charge determination of synthetic cationic polyelectrolytes by colloid titration. *Colloids Surf. A Physicochem. Eng. Asp.* 159 (1), 165–179.
- Kong, Y., Ma, Y., Ding, L., Ma, J., Zhang, H., Chen, Z., Shen, J., 2021. Coagulation behaviors of aluminum salts towards humic acid: detailed analysis of aluminum speciation and transformation. *Separ. Purif. Technol.* 259, 118137.
- Lama, S., Pappa, M., Brandão Watanabe, N., Formosa-Dague, C., Marchal, W., Adriaensens, P., Vandamme, D., 2024. Interference of extracellular soluble algal organic matter on flocculation-sedimentation harvesting of chlorella sp. *Bioresour. Technol.* 411, 131290.
- Li, D., Zhu, L., Wu, Q., Chen, Y., Wu, G., Zhang, H., 2023. Effect of pH treatment on physical stability and antioxidant activity of buckwheat protein/soybean polysaccharide nanocomplex embedded pterostilbene. *Food Biosci.* 55, 102977.
- Li, L., Yu, T., Cheng, S., Li, J., Li, C., Wang, G., Tan, D., Li, L., Zhang, H., Zhang, X., 2022. Removal of cyanobacteria using novel pre-pressurized coagulation: the effect of cellular properties and allogenetic organic matter characteristics. *Separ. Purif. Technol.* 282, 119927.
- Lin, J.-L., Hua, L.-C., Wu, Y., Huang, C., 2016. Pretreatment of algae-laden and manganese-containing waters by oxidation-assisted coagulation: effects of oxidation on algal cell viability and manganese precipitation. *Water Res.* 89, 261–269.
- Liu, B., Gao, Y., Pan, J., Feng, Q., Yue, Q., Guo, K., Gao, B., 2022. Coagulation behavior of polyaluminum-titanium chloride composite coagulant with humic acid: a mechanism analysis. *Water Res.* 220, 118633.
- Liu, C., Ersan, M.S., Wagner, E., Plewa, M.J., Amy, G., Karanfil, T., 2020. Toxicity of chlorinated algal-impacted waters: formation of disinfection byproducts vs. reduction of cyanotoxins. *Water Res.* 184, 116145.
- López, J., Imperial, S., Valderrama, R., Navarro, S., 1993. An improved bradford protein assay for collagen proteins. *Clin. Chim. Acta* 220 (1), 91–100.
- Lui, Y.S., Qiu, J.W., Zhang, Y.I., Wong, M.H., Liang, Y., 2011. Algal-derived organic matter as precursors of disinfection by-products and mutagens upon chlorination. *Water Res.* 45 (3), 1454–1462.
- Ma, L., Peng, F., Lu, Y., Yang, Z., Qiu, B., Li, H., 2022. The effect of coagulation on the removal of algenic organic matter and the optical parameters for predicting disinfection byproducts. *Separ. Purif. Technol.* 280, 119906.
- Naceradska, J., Novotna, K., Cermakova, L., Cajthaml, T., Pivokonsky, M., 2019a. Investigating the coagulation of non-proteinaceous algal organic matter: optimizing coagulation performance and identification of removal mechanisms. *J. Environ. Sci.* 79, 25–34.
- Naceradska, J., Pivokonska, L., Pivokonsky, M., 2019b. On the importance of pH value in coagulation. *J. Water Supply Res. Technol. - Aqua* 68 (3), 222–230.
- Nie, Y., Zhang, R., Li, S., Xia, W., Ma, J., 2023. Removal of microcystis aeruginosa and its extracellular organic matters by using covalently bonded coagulant: an alternative choice in enhanced coagulation for algae-polluted water treatment. *J. Clean. Prod.* 419, 138337.
- Peng, Y., Yang, X., Huang, H., Su, Q., Ren, B., Zhang, Z., Shi, X., 2023. Fluorescence and molecular weight dependence of disinfection by-products formation from extracellular organic matter after ultrasound irradiation. *Chemosphere* 323, 138279.
- Qian, Y., Yu, M., Zhang, R., Wang, Z., 2024. Impact of permanganate with polyaluminium chloride on algae-laden karst water: behaviors and disinfection by-products control. *Environ. Res.* 262, 119758.
- Qu, F., Liang, H., He, J., Ma, J., Wang, Z., Yu, H., Li, G., 2012. Characterization of dissolved extracellular organic matter (dEOM) and bound extracellular organic matter (bEOM) of microcystis aeruginosa and their impacts on UF membrane fouling. *Water Res.* 46 (9), 2881–2890.
- Quang Viet, L., Lee, M.-H., Hur, J., 2019. Using fluorescence surrogates to track allogenetic dissolved organic matter (AOM) during growth and coagulation/flocculation processes of green algae. *J. Environ. Sci.* 79, 311–320.
- Raeke, J., Lechtenfeld, O.J., Wagner, M., Herzsprung, P., Reemtsma, T., 2016. Selectivity of solid phase extraction of freshwater dissolved organic matter and its effect on ultrahigh resolution mass spectra. *Environ. Sci.: Process. Impacts* 18 (7), 918–927.
- Reid, E., Igou, T., Zhao, Y., Crittenden, J., Huang, C.-H., Westerhoff, P., Rittmann, B., Drewes, J.E., Chen, Y., 2023. The minus approach can redefine the standard of practice of drinking water treatment. *Environ. Sci. Technol.* 57 (18), 7150–7161.
- Ren, B., Weitzel, K.A., Duan, X., Nadagouda, M.N., Dionysiou, D.D., 2022. A comprehensive review on algea removal and control by coagulation-based processes: mechanism, material, and application. *Separ. Purif. Technol.* 293, 121106.
- Roselet, F., Vandamme, D., Roselet, M., Muylaert, K., Abreu, P.C., 2017. Effects of pH, salinity, biomass concentration, and algal organic matter on flocculant efficiency of synthetic versus natural polymers for harvesting microalgae biomass. *Bioenergy Res.* 10 (2), 427–437.
- Roth, B.L., Poot, M., Yue, S.T., Millard, P.J., 1997. Bacterial viability and antibiotic susceptibility testing with SYTOX green nucleic acid stain. *Appl. Environ. Microbiol.* 63 (6), 2421–2431.
- Ruan, X., Xiang, Y., Shang, C., Cheng, S., Liu, J., Hao, Z., Yang, X., 2021. Molecular characterization of transformation and halogenation of natural organic matter during the UV/chlorine AOP using FT-ICR mass spectrometry. *J. Environ. Sci.* 102, 24–36.
- Sha, J., Lu, Z., Ye, J., Wang, G., Hu, Q., Chen, Y., Zhang, X., 2019. The inhibition effect of recycled Scenedesmus acuminatus culture media: influence of growth phase, inhibitor identification and removal. *Algal Res.* 42, 101612.
- Vandamme, D., Beuckels, A., Vadelius, E., Depraetere, O., Noppe, W., Dutta, A., Fouberet, I., Laurens, L., Muylaert, K., 2016. Inhibition of alkaline flocculation by algal organic matter for Chlorella vulgaris. *Water Res.* 88, 301–307.
- Wang, B., Zhang, Y., Qin, Y., Li, H., 2021. Removal of microcystis aeruginosa and control of algal organic matter by Fe(II)/peroxymonosulfate pre-oxidation enhanced coagulation. *Chem. Eng. J.* 403, 126381.
- Wang, G., Shi, W., Ma, D., Gao, B., 2020. Impacts of permanganate/bisulfite pre-oxidation on DBP formation during the post chlorine disinfection of ciprofloxacin-contaminated waters. *Sci. Total Environ.* 731, 138755.
- Wang, H., Yang, Y., Zhou, Z., Li, X., Gao, J., Yu, R., Li, J., Wang, N., Chang, H., 2022. Photocatalysis-enhanced coagulation for removal of intracellular organic matter from microcystis aeruginosa: efficiency and mechanism. *Separ. Purif. Technol.* 283, 120192.
- Wang, X., Gan, Y., Guo, S., Ma, X., Xu, M., Zhang, S., 2018. Advantages of titanium xerogel over titanium tetrachloride and polytitanium tetrachloride in coagulation: a mechanism analysis. *Water Res.* 132, 350–360.
- Xu, J., Zhao, Y., Gao, B., Han, S., Zhao, Q., Liu, X., 2018. The influence of algal organic matter produced by microcystis aeruginosa on coagulation-ultrafiltration treatment of natural organic matter. *Chemosphere* 196, 418–428.
- Yang, X., Zheng, X., Wu, L., Cao, X., Li, Y., Niu, J., Meng, F., 2018. Interactions between algal (AOM) and natural organic matter (NOM): impacts on their photodegradation in surface waters. *Environ. Pollut.* 242, 1185–1197.
- Yan, Y., Zhan, H., Wang, X., 2020. Formation characteristics of disinfection by-products from algal organic matter in ozonation/chlorine disinfection. *China Water & Wastewater* 36 (5), 7–13.
- Yu, M., Qian, Y., Ni, M., Wang, Z., Zhang, P., 2024. Algae removal and algal organic matter chemistry modulated by KMnO₄-PAC in simulated karst water. *Chemosphere* 354, 141733.
- Zhang, X., Zhang, H., Liu, Q., Li, L., Li, L., Zhang, X., 2020. Harvesting of microcystis flos-aquae using chitosan coagulation: influence of proton-active functional groups originating from extracellular and intracellular organic matter. *Water Res.* 185, 116272.
- Zhang, K., Qiu, C., Cai, A., Deng, J., Li, X., 2020. Factors affecting the formation of DBPs by chlorine disinfection in water distribution system. *Desalination Water Treat.* 205, 91–102.
- Zhang, Y., Lu, Z., Zhang, Z., Shi, B., Hu, C., Lyu, L., Zuo, P., Metz, J., Wang, H., 2021. Heterogeneous Fenton-like reaction followed by GAC filtration improved removal efficiency of NOM and DBPs without adjusting pH. *Separ. Purif. Technol.* 260, 118234.